

Deep Learning-Based Plant Organ Segmentation and Phenotyping of Sorghum Plants Using LiDAR Point Cloud

Ajay Kumar Patel^{ID}, Student Member, IEEE, Eun-Sung Park^{ID}, Hongseok Lee^{ID}, G. G. Lakshmi Priya^{ID}, Hangi Kim^{ID}, Rahul Joshi^{ID}, Muhammad Akbar Andi Arief^{ID}, Moon S. Kim^{ID}, Insuck Baek^{ID}, and Byoung-Kwan Cho^{ID}

Abstract—Increasing food demands, global climatic variations, and population growth have spurred the growth of crop yield driven by plant phenotyping in the age of Big Data. High-throughput phenotyping of sorghum at each plant and organ level is vital in molecular plant breeding to increase crop yield. LiDAR (light detection and ranging) sensor provides 3-D point clouds of plants with the advantages of high precision, high resolution, and rapid measurement. However, need to develop robust algorithms for extracting the phenotypic traits of sorghum plants using LiDAR 3-D point cloud. This study utilized four 3-D point cloud-based deep learning models named PointNet, PointNet++, PointCNN, and dynamic graph CNN for the specific objective of the segmentation of sorghum plants. Subsequently, phenotypic traits were extracted using the segmentation results. Study plants sample were grown under controlled conditions at various developmental stages. The extracted phenotypic traits outcome has been validated through the manually measured phenotypic traits of the sorghum plant. PointNet++ outperformed the other three deep learning models and provided the best segmentation result with a mean accuracy of 91.5%. The correlations of the six phenotypic traits, such as plant height, plant crown diameter, plant compactness, stem diameter, panicle length, and panicle width were calculated from the segmentation results of the PointNet++ model and the measured coefficient of determination (R^2) were 0.97, 0.96, 0.94, 0.90, 0.95,

Manuscript received 20 April 2023; revised 8 July 2023 and 23 August 2023; accepted 27 August 2023. Date of publication 7 September 2023; date of current version 20 September 2023. This work was supported in part by the National Institute of Crop Science under Project PJ0156892021 of the Rural Development Administration, Republic of Korea. (Corresponding author: Byoung-Kwan Cho.)

Ajay Kumar Patel, Eun-Sung Park, Hangi Kim, and Muhammad Akbar Andi Arief are with the Department of Smart Agricultural Systems, College of Agricultural and Life Science, Chungnam National University, Daejeon 34134, South Korea (e-mail: apatel1@ce.iitr.ac.in; sung12022002@hanmail.net; zx-cvkhk@gmail.com; m.akbar.andi@mail.ugm.ac.id).

Hongseok Lee is with the National Institute of Crop Science, Rural Development Administration, Miryang 50424, South Korea (e-mail: ehg117@korea.kr).

G. G. Lakshmi Priya and Rahul Joshi are with the Department of Biosystems Machinery Engineering, College of Agricultural and Life Science, Chungnam National University, Daejeon 34134, South Korea (e-mail: lakshmi.priya.gg@vit.ac.in; rahul.joshi98@yahoo.com).

Moon S. Kim and Insuck Baek are with the Agricultural Research Service, United States Department of Agriculture, Environmental Microbial and Food Safety Laboratory, Beltsville, MD 20705 USA (e-mail: moon.kim@usda.gov; insuck.baek@usda.gov).

Byoung-Kwan Cho is with the Department of Smart Agricultural Systems, College of Agricultural and Life Science, Chungnam National University, Daejeon 34134, South Korea, and also with the Department of Biosystems Machinery Engineering, College of Agricultural and Life Science, Chungnam National University, Daejeon 34134, South Korea (e-mail: chobk@cnu.ac.kr).

Digital Object Identifier 10.1109/JSTARS.2023.3312815

and 0.88, respectively. The obtained results showed that LiDAR 3-D point cloud have good potential to measure the sorghum plant phenotype traits rapidly and accurately using deep learning techniques.

Index Terms—3-D point cloud, deep learning, lidar technique, phenotyping, sorghum.

I. INTRODUCTION

S ORGHUM (*Sorghum bicolor* L. Moench) is essential in providing nutrition to humans, especially in areas with low rainfall. Under the influence of global climate change, the world's population is increasing while the area of arable land is decreasing, placing unprecedented strain on food production and farmers' livelihood security. The study of plant growth processes plays an important role in modern agriculture. Plant genotypic and phenotypic techniques are important in accelerating breeding programs to meet the growing food and energy needs [1]. Genotyping techniques are well developed, and the shortcomings of “low efficiency” and “long-term” traditional breeding methods based on human experience have been successfully resolved [2]. The Phenotypic technique is a fast-growing field of plant science, which is used to analyze and measure the phenotype change in response to genotype and environment on an organism. It helps in developing a high-throughput (HTP) phenotyping platform, which can accelerate precise breeding and hence improve the crop yields [3], [4].

Phenotypic data of high quality is essential to plant breeders and scientists. Such as phenotypic measurements of traits related to plant architecture are helpful for understanding the relationship of genotype-phenotype-environment influenced by plant architecture. A plant's architecture refers to the sets of traits that denotes the 3-D arrangement of plant organs [5], and it is essential for determining their phenotyping [6]. Generally, measurements of phenotypic traits associated with plant architecture, such as plant height, crown diameter, plant compactness, stem diameter, etc., are often manually collected. These manually collected phenotypic traits are time-consuming, labor-intensive, prone to human errors, inefficient, and subjective. As a result, there is often a scarcity of high-quality phenotypic data. Therefore, it is crucial to develop an automated, precise, and non-destructive technique for extracting features of phenotypic

traits, especially at holistic and component plant levels, with greater efficiency and precision.

The emergence of machine vision imaging methods has immensely promoted the burgeoning of image-analysis-based HTP phenotypic traits extraction [7]. Imaging-based phenotypic traits extraction methods have been widely used to obtain the specific morphological plant traits [8], rice panicle traits and detection [9], root traits [10], yield-related traits [11], crop canopy cover [12], crop plant growth and drought-responsive traits [13], and plant disease detection [14]. Extensive reviews on the use of image-based plant phenotyping for extraction of phenotypic traits can be found in [15], [16], and [17]. These imaging-based approaches can provide 2-D information with extremely high spatial resolution at a reasonable cost. However, the limitations of these imaging methods are the data obtained from images is 2-D and subject to illumination and occlusion induced by leaves when collecting images from different directions [7]. Also, due to the lack of a third dimension, these imaging techniques fail to acquire volumetric and areal information [18]. Although stereo images and multiple-view can rebuild the 3-D shape of a plant, but the limitations of the image remain extant [19]. The image-based 3-D construction worked well in a controlled condition, but it lost volumetric and precise spatial data under a field environment. It could not avoid the tradeoff between efficiency and accuracy [20]. Therefore, imaging-based techniques still have constraints in acquiring highly precise 3-D phenotypic traits. In contrast, the 3-D active remote sensing technology called light detection and ranging (LiDAR) enables recording of 3-D point clouds, providing a comprehensive depiction of essential spatial information and 3-D depth in millimeter detail. LiDAR has been widely used in ecological studies and quantitative forestry throughout the last few decades [21]. The widespread utilization of 3-D LiDAR point cloud data in agricultural applications has effectively addressed data occlusion and overlapping challenges. This technology plays a crucial role in enabling high-precision phenotyping in agriculture, exhibiting significant potential in crop organ segmentation and phenotyping, and offering promising prospects for advancements in plant phenotyping [22], [23], [24], [25], [26], [27], [28], [29], [30], [31], [32], [33], [34], [35]. Extensive investigation in LiDAR's recent advances and future prospects on plant phenomics for plant breeding and management and applications in precision agriculture can be found in [36] and [37]. Plant phenotypic studies based on LiDAR at plant organ (i.e., leaf and stem) levels are still in the preliminary stage. The lack of an accurate plant organ segmentation method and automatic phenotypic trait extraction techniques for crops may be the main bottleneck.

Over the last few years, the application based on computer vision methods has made substantial progress in acquiring HTP plant phenotype data [38], [39]. Images of soybean plants were collected using an image-based HTP phenotyping platform, and the performance of machine learning methods in segmenting nonoverlapped and overlapped soybean plants was evaluated in [40]. A comprehensive overview of the latest studies utilizing deep convolutional neural networks in the field of plant phenotyping applications has been presented in [17]. Zhou et al. [41] proposed a deep learning-based maize image analysis software

named Maize-IAS for HTP plant phenotyping. A thorough review of the recent developments in deep learning applications for HTP was presented in [42]. Recently, Cardellicchio et al. [43] utilized single-stage detectors based on YOLOv5 to detect tomato plants phenotyping traits. Extensive reviews on current machine vision methods for plant trait classification and estimation and 3-D computer vision techniques in food and agriculture applications can be found in [44], [45], and [46]. These technologies make it easier to acquire phenotypic traits such as plant color, morphology, texture, and structure efficiently and accurately [47] and avoid the drawbacks of traditional plant phenotyping procedures [48]. Fast data acquisition and 3-D phenotyping have been made possible because of the rapid advancements in sensor technology and the enhancement in computing power [16], [49], [36]. For example, the 3-D plant data have been acquired for phenotyping using depth cameras [50], [51], LiDAR [23], and multiview imaging methods [32], [52], [53]. And various phenotypic traits, including stem height, leaf inclination, plant volume, and leaf area, can be extracted using these technologies [54], [55], [28]. Segmenting a 3-D point cloud data of a shoot to multiorgans at the individual or organ plant level is one of the bottlenecks in 3-D plant phenotypic investigations [6], [56], [57]. Several 3-D data segmentation techniques are currently available for plants, most of which primarily focus on individual [58] and population scales [59], for instance, threshold-based [60], geometry-based [61], and machine learning techniques [62]. These necessitate a lot of manual interaction, particularly based on the geometry and threshold approaches.

The segmentation results of plant phenotyping investigations rely on the empirical parameters settings, which cannot handle the huge amount of data processing [22]. Generally, most existing 3-D data processing techniques for plants are tedious and involve numerous manual interactions, which results in accumulating a large amount of raw data. In addition, these approaches limit the HTP resolution of the phenotypic indicators useful to agronomists. Therefore, developing an accurate, efficient, and noninvasive technique is essential to enhance the HTP and automatic plant-to-organ segmentation of plant 3-D point cloud data [63], [64]. Machine learning-based algorithms can automatically extract features from Big Data sets [24], [65], especially deep learning techniques, which have opened new possibilities for overcoming these issues [29], [66], [67], [68], [69]. Deep learning approaches for 3-D plant data processing and phenotypic measurements are challenging but promising [64], [70]. Deep learning-based plant-organ segmentation of 3-D point cloud is a relatively new emerging research area, [47], [71], [72], [73], [69], [74], [75], [76]. So far, 3-D point cloud-based deep learning has emerged as a promising technique for achieving high-precision plant organ segmentation and phenotypic traits extraction from plant point cloud datasets.

The objective of this research is the sorghum plant-organ (stem-leaf-panicle) segmentation from LiDAR 3-D point cloud data using four deep learning models, i.e., PointNet, PoinNet++, PointCNN, and DGCNN. Subsequently, the extraction of sorghum plant phenotype traits using the

segmentation results. The accuracy assessment of the output was carried out using manually measured information of sorghum plants' phenotypic traits. The main research contributions are as follows:

- 1) A well-labeled sorghum point cloud dataset for stem-leaf-panicle segmentation was built. The labeled dataset contains 800 plant samples generated from 500 individual sorghum plant point clouds through data augmentation with manual labels under several growth periods covering 30 days.
- 2) Addressed the application of four deep learning models mentioned above for automatically segmenting sorghum plant organs (stem-leaf-panicle) from 3-D LiDAR point cloud data.
- 3) Measured the six important sorghum plant phenotyping traits such as plant height, plant crown diameter, plant compactness, stem diameter, panicle length, and panicle width from the segmented point clouds.

This research showcases the potential of 3-D deep learning models in achieving precise and efficient segmentation of sorghum plant organs and phenotyping traits extraction, laying the foundation for automated sorghum plant phenotyping tasks.

II. RELATED WORK

A. Point Cloud Segmentation and Phenotyping

The automatic segmentation of plant organs from accurate point cloud data is essential to extracting high-precision phenotypic traits and high throughput. Conventional segmentation methods such as the normal difference [77], octree algorithm [78], and 3-D skeleton [22] typically employed hand-crafted features for plant organ segmentation from 3-D LiDAR point clouds data. To segment stem and leaf instances of individual maize plants from LiDAR point cloud data, Jin et al. [22] introduced a median normalized-vector growth algorithm. This algorithm directly operated on point cloud data and was inspired by various sources, including the L1-median algorithm, theory of density-based spatial clustering of applications with noise, and Newton's first law. In paper [34] automatic method was proposed for the segmentation of maize organs, encompassing skeleton extraction, coarse segmentation using the extracted skeleton, and fine segmentation relying on stem-leaf classification. In paper [33] a robust method was presented that effectively achieved the segmentation of maize organs and enabled the extraction of maize architectural traits using LiDAR point clouds data. Although these methods can manage plants with uncomplicated structures through labor-intensive and meticulous parameter tuning, however, they still exhibit limitations regarding their ability to generalize and accurately segment various crop species with distinct canopy structures and leaf shapes.

The recent advancements in 3-D-based deep learning methods demonstrate significant potential in enhancing the generalization and accuracy of plant organ segmentation [76], [79]. This progress can be attributed to extracting complex plant structural information from large-scale with high-dimensional point cloud datasets, high-performance hardware, and advancements in neural network architectures [80]. Deep learning-based methods utilize labeled point clouds data to learn the features and make

decisions simultaneously from an incorporated deep neural network. This capability enables the optimization of feature extraction and decision-making processes jointly, leading to enhance overall segmentation performance. Many studies have employed deep learning networks to extract significant point cloud features essential for semantic and instance segmentation of plant organs in recent years [18], [35], [68], [71], [75], [76], [29], [81].

In paper [29], the combined deep learning (Fast R-CNN) and regional growth methods were presented for the segmentation of individual maize plants using point clouds obtained from terrestrial LiDAR scanning. A voxel-based convolutional neural network for the classification and segmentation of maize stems and leaves have introduced by [71]. In [70], Boogaard et al. demonstrated the potential of a deep learning-based segmentation method for partially complete 3-D point clouds of cucumber plants. In [67], Ao et al. proposed convolutional neural networks and a morphological characteristics-based approach for the segmentation of stems and leaves of individual maize plants in their natural growth conditions. Li et al. [68] introduced an automatic approach named DeepSeg3DMaize for the segmentation of maize plants' 3-D point clouds. DeepSeg3DMaize has utilized high-throughput data acquisition techniques and deep neural networks to segment maize plant organs accurately and efficiently. In [82] a plant point cloud segmentation network was proposed named MASPC_Transform that was based on the separation of multihead attention and position code techniques. Deep learning networks PlantNet [76] and PSegNet [75] were designed for the semantic segmentation of plant organs and leaf instance segmentation using manually labeled points cloud dataset of multiple plant species including tobacco, tomato, and sorghum. Turgut et al. [74] evaluated the impact of synthetic rosebush plant data on the performance of 3-D point-based deep learning architectures and performed the real rosebush plants segmentation into their organs. A 3-D point-based deep learning network called RoseSegnet was introduced by Turgut et al. [83], designed explicitly for segmenting point clouds of rosebush plants into their structural parts. Recently, Wang et al. [35] developed a distance field-based segmentation pipeline to enable rapid plant organ location and segmentation. Marks et al. [84] proposed an approach for segmenting leaves from point clouds recorded in real field conditions for plant phenotyping. Du et al. [79] proposed a 3-D point cloud deep learning-based network plant segmentation transformer and performed the rapeseed plants semantic segmentation.

III. MATERIALS AND METHODS

A. Experimental Design and Data Acquisition

The experiments were conducted on sorghum plants. These plants were grown in a growth chamber (greenhouse) at Chungnam National University, as shown in Fig. 1. A total of 140 well-planted sorghum samples were chosen and transplanted into pots. The 3-D LiDAR points cloud of all study samples was acquired using a Leica BLK360 Imaging scanner (Leica Geosystems, Heerbrugg, Switzerland). The technical specifications of the LiDAR system are shown in Table I.

TABLE I
TECHNICAL SPECIFICATIONS OF LEICA BLK360

Leica BLK360		Specifications
		Scanning unit
Wavelength	830 nm	
Operational range	minimum 0.6m - up to 60 m	
Dimensions	Height: 165 mm / Diameter: 100 mm	
Field of View	Horizontal 360° Vertical 300°	
Acquisition speed	up to 360.000 points/sec	
Ranging accuracy	4 mm @ 10 m / 7 mm @ 20 m	
3D point accuracy	6 mm @ 10 m / 8 mm @ 20 m	
Distance measurement method	Pulse transit time with waveform digitizing	
Camera unit (Imaging)		
RGB camera system	15 megapixels, 3-camera system, FOV: Horizontal 360° Vertical 300°	
Thermal camera	Thermal panoramic image, FOV: Horizontal 360° Vertical 70°	



Fig. 1. Sorghum plants in green house.

Sorghum plants' 3-D points cloud, and their manually measured phenotypic traits were acquired under indoor conditions. After taking point cloud data and RGB images, plant phenotypic traits were manually measured with standard techniques to evaluate the performance of the approach. The ground truth data was collected on the same day. Plant height was measured from the stem emerging from the soil to the top position of the plant using a measuring tape. The plant crown diameter was measured using a measuring tape. Panicle length was measured from the top position of stem to the top position of the panicle using a measuring tape. The stem diameter and panicle width were measured using a caliper at the stem section. 3-D LiDAR point cloud data processing steps were developed for determining plant organ segmentation and plant phenotypic traits. Fig. 2 expresses the overall workflow of the proposed approach.

B. Point Cloud Data Preprocessing

The irregularity of the point cloud data structure makes point cloud analysis challenging [85]. Since raw point cloud data contains some unwanted noise and artifacts, denoising and downsampling were performed to enhance accuracy and processing speed. The downsampling was performed to remove the redundant points from the input point cloud data. The point cloud density of each plant was reduced after downsampling. It was observed that the downsampled point clouds retained the phenotypic traits of study plants and were sufficient for efficiently obtaining the plant phenotypic traits. The input point

cloud data was normalized after the downsampling. Feature scaling or normalization is an essential preprocessing step in computer vision-based algorithms because this encloses all features within a common boundary without causing any information loss. Annotating point clouds is crucial in applying deep learning for plant organ segmentation since it labels the data and allows for efficient model training. Annotating large-scale plant point clouds point by point is a highly time-intensive process, and a user-friendly annotation toolkit is presently lacking. Pointwise annotation was conducted on input point clouds to prepare a labeled dataset for segmenting different sorghum plant-organ. Each sorghum plant's leaf, stem, and panicle were manually labeled in 0, 1, and 2, respectively, using the *segment* module of the CloudCompare software [86] as illustrated in Fig. 3 (annotated point cloud). The proposed approach comprised the following four sections:

- 1) point cloud data preprocessing and annotation;
- 2) deep learning-based plant organ (stem-leaf-panicle) segmentation;
- 3) phenotypic traits extraction;
- 4) accuracy assessment.

Fig. 3 shows the illustration of the proposed approach.

C. Deep Learning Architectures Based on 3-D Point Cloud

In this study, four noteworthy deep learning models based on 3-D point clouds have been applied for the challenge of organ (stem-leaf-panicle) segmentation of sorghum plants, those are as follows:

- 1) PointNet [87];
- 2) PointNet++ [88];
- 3) PointCNN [89];
- 4) dynamic Graph CNN (DGCNN) [90].

The design parameters of the four networks, including the number of features and layers and other hyperparameters like the radii of local regions, were initially set in their default settings for 3-D point cloud datasets that contain scenes of indoor locations. The standard procedure for adjusting these parameters

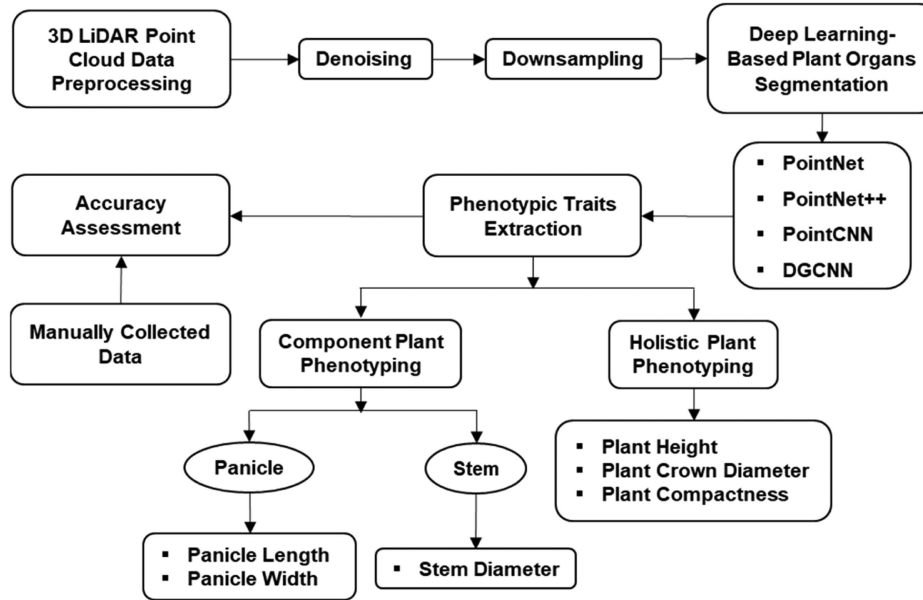


Fig. 2. Main steps of the proposed approach for plant phenotypic traits extraction.

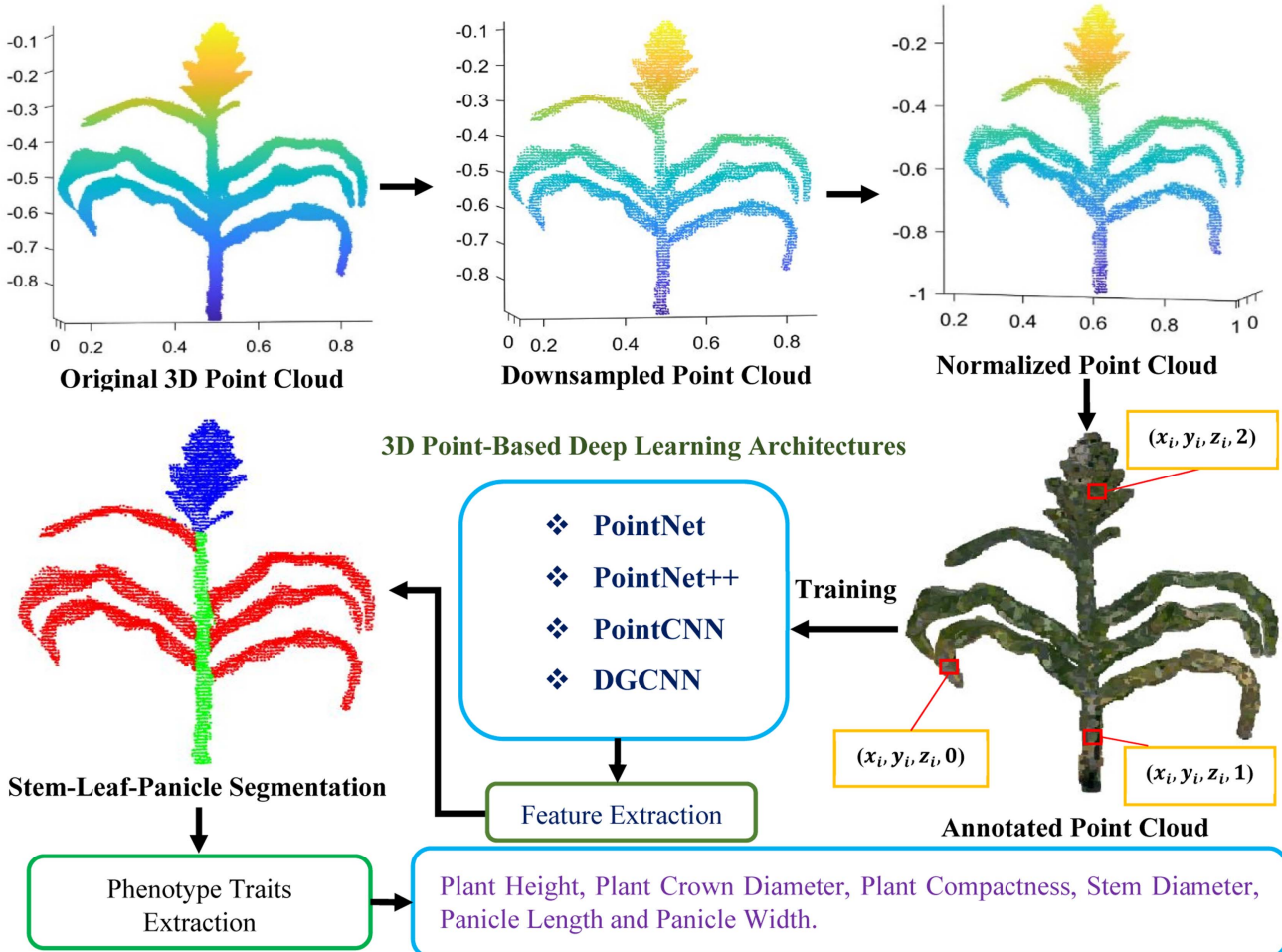


Fig. 3. Illustration of the methodology workflow.

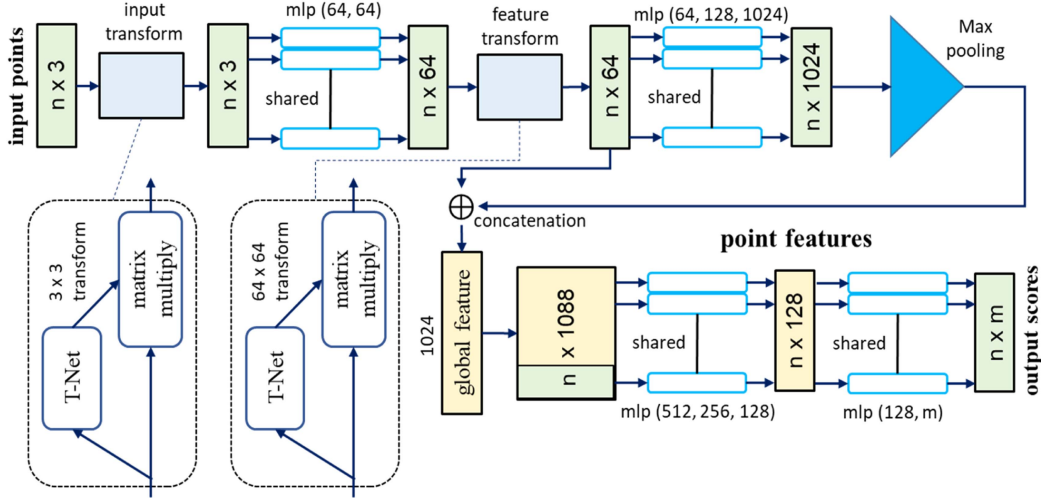


Fig. 4. Architecture of the PointNet model for 3-D point cloud segmentation.

is to experiment with different settings on a validation set to find the ones that perform the best. In this article, the default architecture settings of all four models, including feature extraction at each layer and hyper-parameters, remained unchanged during the plant organ segmentation. Plant self-similar and multiscale characteristics must be considered while creating a 3-D point-based architecture to function well on plant data [74]. The architecture should support the network's many fields of receptivity in hierarchical order, and their sizes should be simple to adjust to the scales of different plant structures. The salient approaches of these deep learning architectures to the challenge of encoding the 3-D point clouds' local geometric structure have been described in the following sections. The parameters of the architectures that produced the best results have been presented. Please refer to the source articles for more detailed information on the architectures' default structures and other characteristics.

1) *PointNet*: In [87], Charles et al. proposed the first deep neural network architecture called PointNet, which directly processes the raw point cloud data as input. Each 3D point's (x , y , z) coordinates are transformed separately into high-dimensional features by multilayer perceptrons (MLP) with shared parameters. All the point features associated with fully connected MLPs are summarized using a single maximum pooling operation. A single global feature vector describes the input point cloud as a result. Individual features based on points are concatenated from this feature vector and processed by subsequent layers. MLP layers with shared weights are employed to the concatenated features to determine the scores of a class for each point. Fig. 4 shows the PointNet architecture for the segmentation of 3-D point cloud data. The PointNet architecture learns features pointwise independently through several MLP layers and uses a max-pooling layer to extract the global features. Since each point in PointNet learns features independently, therefore the final predictions are primarily influenced by the points' locations rather than the organization of local geometric structures. Furthermore, it cannot capture information about the local geometric structures between the points.

2) *PointNet++*: In [88], Qi et al. proposed a hierarchical network called PointNet++, which can capture the delicate geometric structures from each point's neighborhood. It was designed to summarize the features based on the point at different local scales rather than at a global level. The input point clouds were divided into overlapping local areas, the real PointNet architecture was employed in these areas, and a feature vector was generated that captured the geometric structure of the local neighborhood. The feature extraction and grouping were done in a hierarchical order. The architecture of PointNet++ is composed of two sorts of layers: 1) set abstraction (SA) layer and 2) feature propagation (FP) layer. Sampling and grouping are the two stages of the SA layer. The furthest point sampling algorithm was used to select F representative points during the sampling stage. A local neighborhood with a defined radius R was generated around each representative point during the grouping stage; consequently, local groups overlap. M points were chosen at random to form a group in this neighborhood. The PointNet architecture was employed in each group separately to extract summarized features across all points in the group. Feature vectors based on the group to the input point cloud's original points were propagated through the FP layers. Interpolation from the features of a point's nearest neighbors was used to propagate features to that point. The PointNet architecture was applied to revise the features of each point by integrating interpolated and existing features from the SA stage. Fig. 5 shows the PointNet++ architecture for the segmentation of 3-D point cloud data. The set abstraction layer takes an $N \times (d + C)$ matrix as input, where N denotes the number of sample points, d is the dimension of the coordinates of the points, C is the dimension of the point features, and K denotes the number of points in the centroid points neighborhood.

3) *PointCNN*: In [89], Li et al. introduced a deep learning architecture called PointCNN. This architecture was a generalization of CNN that takes advantage of spatially local correlation from point cloud data. A convolution operator defined as X-Conv has been presented in PointCNN architecture. This operator weights and permutes the neighbors' feature of input

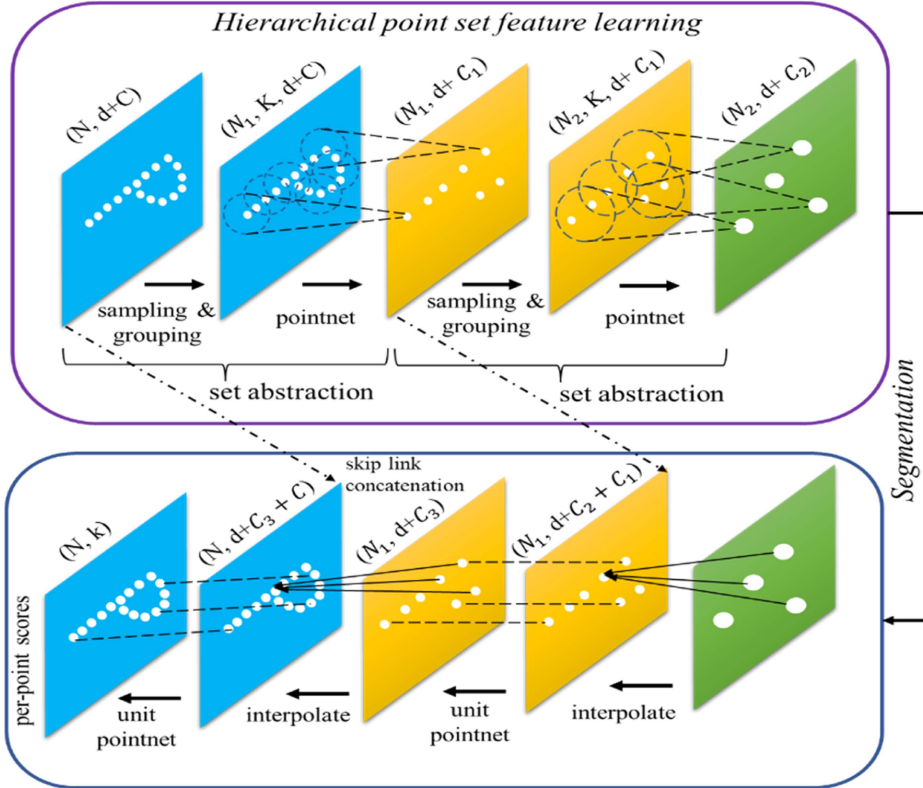


Fig. 5. Demonstration of hierarchical feature learning PointNet++ architecture for 3-D point cloud segmentation.

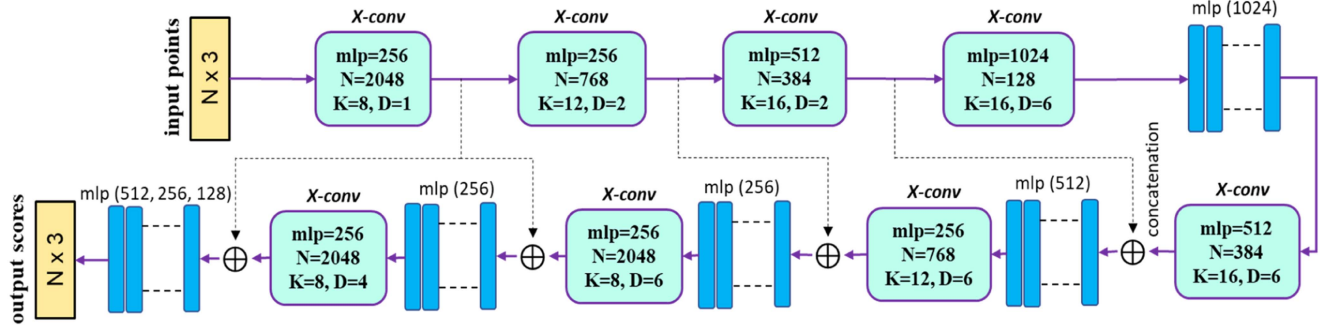


Fig. 6. PointCNN architecture for 3D point cloud segmentation.

points before a standard convolution processes them. In the X-Conv process, a transformation matrix of sized $K \times K$ was predicted for K nearest neighbors' points with MLPs. Then the standard convolution layers were employed for the transformed features. The representative points were produced using the farthest point sampling algorithm to define the wide-open fields for convolution. And the features that emerged from the X-conv operator were accumulated from these representative points. When points were dilated by a factor and the X-conv operator was applied hierarchically, then the resulting point features were accumulated into fewer points and represented wider spatial areas. An encoder-decoder structure was used to process the point features for segmentation. Fig. 6 shows the architecture of the PointCNN model for the segmentation of 3-D point cloud data. The nearest neighbors number employed in convolution

was denoted by K , the sampled points number was denoted by N , and the point dilation rate was denoted by D .

4) *Dynamic Graph CNN (DGCNN)*: In [90], Wang et al. proposed a deep learning architecture called DGCNN. It was designed to incorporate the 3-D points' local neighborhood information directly within the network instead of an individual grouping process performed by PointNet++. A graph structure was used to represent a point's local neighborhood. Edge features were extracted using the EdgeConv technique to encode the spatial correlation between the point and its K -nearest neighbors. The MLPs employed for edge representations rather than point locations were used to extract the edge features. In contrast to CNN structures employed in conventional grids, fixed graphs were not applied. In each layer, the K neighborhoods of the point feature changed; therefore, the graphs were

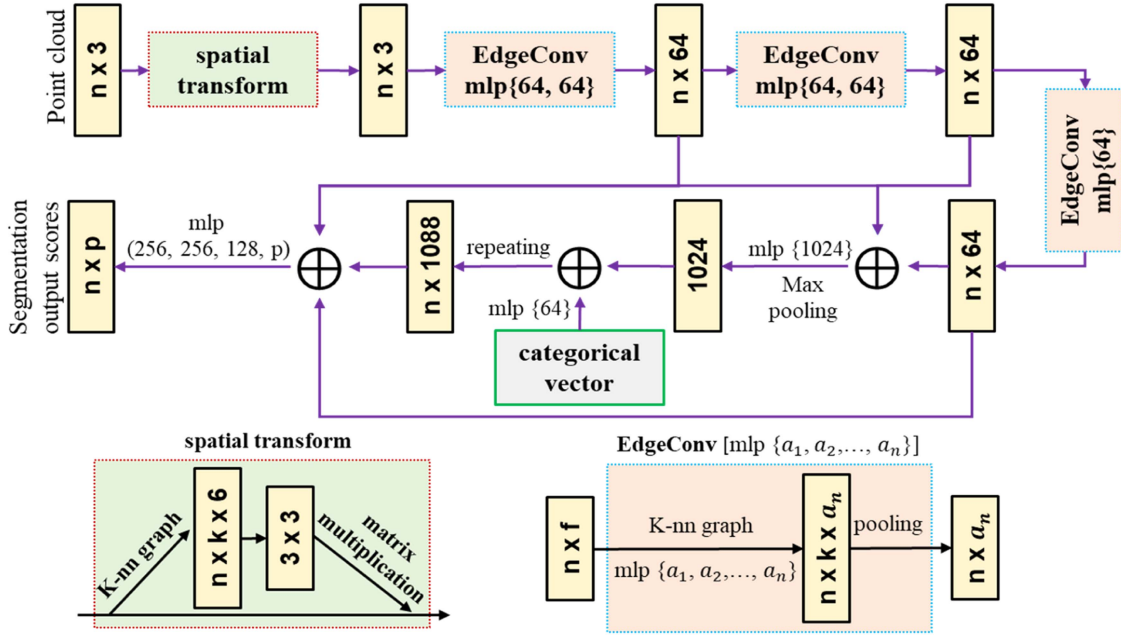


Fig. 7. Architecture of the DGCNN model for 3D point cloud segmentation.

updated. The geometrical closeness between nearest neighbor points was considered only in the first layer of the architecture. In the next layers, the edge representations were constituted between nearest neighbors who were close to each other in the feature space. However, that was advantageous in disseminating information about the closeness in the feature space. The local spatial grouping of a multi-scale hierarchy does not exist in DGCNN. The structure of local geometry was only captured at an extremely localized level, namely within a point's nearest neighbors. Fig. 7 shows the architecture of the DGCNN model for the segmentation of 3D point cloud data.

D. Segmentation Performance Evaluation

The quantitative evaluation of each deep learning model's segmentation results for all predicted points was accomplished using the annotated ground truth data. The plant organ (stem-leaf-panicle) segmentation result was examined for each sorghum plant. Higher true positive (TP_c), lower false positive (FP_c), and lower false negative (FN_c) are generally associated with high accuracy [91]. Where $C \in \{\text{leaf, stem, panicle}\}$ was the class of the organ part of a sorghum plant. Based on the confusion matrix, the four often used evaluation indicators, including recall (R_e), precision (P_r), Intersection over Union (IoU), and F1-score (F) were adopted to evaluate the plant organ segmentation accuracy of each deep learning model. The segmentation evaluation indicators can be defined as follows:

$$R_e = \frac{TP_c}{TP_c + FN_c} \quad (1)$$

$$P_r = \frac{TP_c}{TP_c + FP_c} \quad (2)$$

$$\text{IoU} = \frac{TP_c}{TP_c + FN_c + FP_c} \quad (3)$$

$$F = \frac{2P_r R_e}{P_r + R_e} \quad (4)$$

$$\text{overall accuracy} = \frac{\text{total correctly segmented points}}{\text{total points of each individual sorghum}}. \quad (5)$$

E. Phenotypic Trait Measurement

The segmented plant organ (stem-leaf-panicle) points were used to measure the phenotypic traits at individual sorghum plant level. Six phenotypic traits were measured from the segmented point clouds: plant height, crown diameter, plant compactness, stem diameter, panicle length, and panicle width. There are two types of morphological traits that can be identified in the point cloud data: 1) holistic phenotypic traits and 2) component phenotypic traits. Holistic phenotypic traits evaluate the complete plant structure, like plant height, crown diameter, and plant compactness. Component phenotypic traits examine the individual plant organs, such as stem diameter, panicle length, and panicle width. The sorghum plant height was calculated using the difference between the maximum and minimum (plant stem emerges from the soil) z -coordinate values of the point clouds. Similarly, the panicle length was calculated using the difference between the maximum and minimum z - coordinate values of the segmented point clouds of sorghum panicles. The plant height (H) and panicle length can be estimated using the following equation:

$$H = z_{\max} - z_{\min}. \quad (6)$$

The crown diameter of a sorghum plant was estimated using the difference between the maximum and minimum x - coordinate values of the point clouds. The crown diameter (C_d) can be calculated as follows:

$$C_d = x_{\max} - x_{\min}. \quad (7)$$

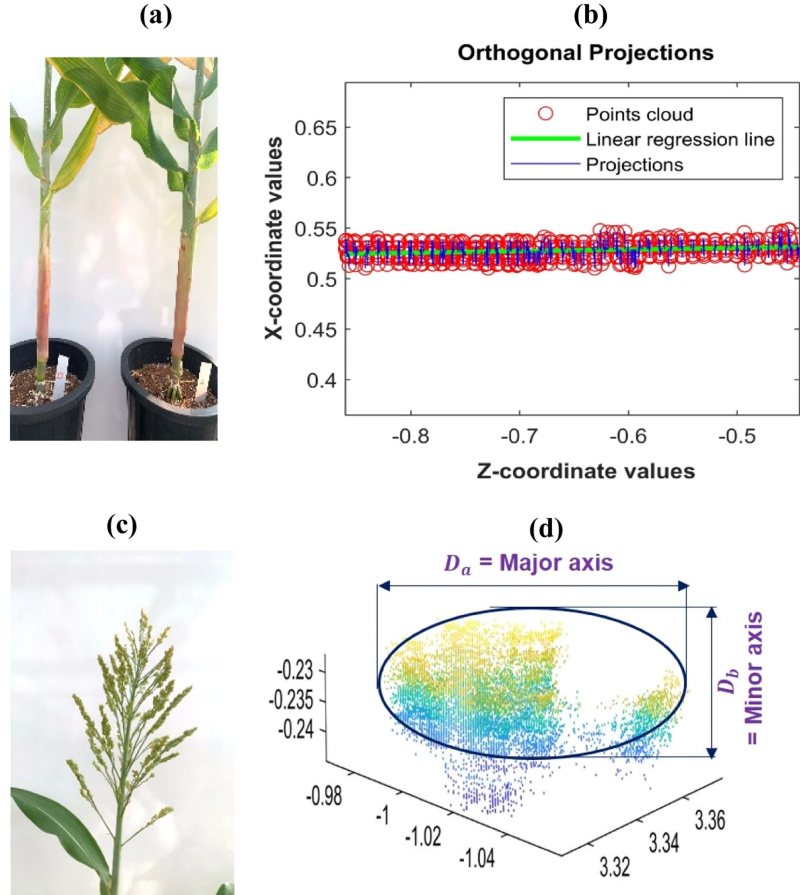


Fig. 8. Phenotypic trait measurement (stem diameter and panicle width). (a) Original stems of sorghum. (b) Straight-line segment was fitted to the stem points cloud using the least squares approach. (c) Original panicle of a sorghum. (d) Orthogonal projection of the sliced panicle points cloud with ellipse fitting.

The plant compactness of a sorghum plant was determined through dividing plant crown diameter by plant height. The plant compactness (C_p) can be calculated as follows:

$$C_p = \frac{C_d}{H}. \quad (8)$$

Stem diameter was computed using the following steps:

- 1) A straight-line segment was fitted to the stem point clouds using the least squares method, as shown in Fig. 8(a) and (b). The line segment's length was equivalent to the stem height.
- 2) All projection distances from the stem points to the line segment were calculated.
- 3) Determined the median of these distances.
- 4) Finally, used twice the median to compute the stem diameter.

In the segmented sorghum panicle points cloud, because of the semi-compact panicles' morphology [see Fig. 8(c)], the four slices of panicle with 1 cm thickness of each slice were used for measurement of the panicle width. The panicle width was estimated based on a roughly elliptical cross-section of the panicle's; hence the points cloud of each panicle slice was orthogonally projected onto the Y - Z plane, as shown in Fig. 8(d). An ellipse fitting operation was then applied to the projected points cloud using built-in functions of the OpenCV library [92].

This function first finds the contour and then approximates an ellipse by reducing the algebraic separation to its constraints [93]. The fitted ellipse's major axis represents the panicle width along the elliptical cross-section's major axis [see Fig. 8(d)]; therefore, the panicle width can be determined by averaging the major axes of all the panicle slices' ellipses.

F. Phenotypic Trait Extraction Evaluation

Linear regression analysis was carried out between the deep learning segmentation model derived measurements and the manual measurements for all extracted phenotypic traits. The root-mean-square error (RMSE), mean absolute percentage error (MAPE), and coefficient of determination (R^2) statistics were calculated to examine the quantitative accuracy of extracted phenotypic traits. RMSE estimates the variations between the predicted and manually measured plant phenotypic traits. MAPE measures the accuracy of a model and R^2 assesses the linear relationships between the predicted and manually measured plant phenotypic traits. These statistical parameters were calculated as follows:

$$\text{RMSE} = \sqrt{\frac{\sum_{i=1}^n (x_i - \hat{x}_i)^2}{n}} \quad (9)$$

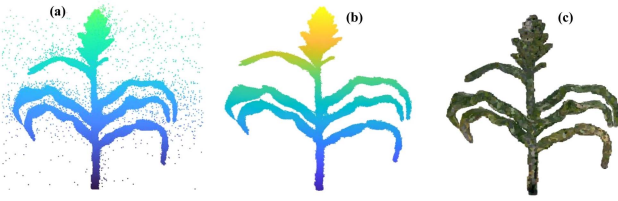


Fig. 9. LiDAR 3-D point cloud data of a sorghum plant. (a) Raw data. (b) Denoised data. (c) Input data.

$$\text{MAPE} = \frac{1}{n} \sum_{i=1}^n \left| \frac{x_i - \hat{x}_i}{x_i} \right| \quad (10)$$

$$R^2 = 1 - \frac{\sum_{i=1}^n (x_i - \hat{x}_i)^2}{\sum_{i=1}^n (x_i - \bar{x})^2} \quad (11)$$

where n represents the total number of plants to be compared, x_i represents the values of manually measured and \hat{x}_i represents the values of phenotypic traits predicted from the deep learning segmentation model for the i th plant, and \bar{x} represents the mean of manually measured results.

IV. RESULTS AND DISCUSSION

The raw input point cloud data as shown in Fig. 9(a) was denoised using the statistical outlier removal tool in open3d. The resultant denoised point cloud of a sorghum plant is shown in Fig. 9(b) and the input data in Fig. 9(c).

A. Stem-Leaf-Panicle Segmentation

Four deep learning models (PointNet, PointNet++, PointCNN, and DGCNN) have been tested to segment sorghum plants to their organs (stem-leaf-panicle). The default architecture settings, including feature extraction at each layer, remained unchanged during the experiments. PointNet, PointNet++, PointCNN, and DGCNN were trained with 100, 201, 100, and 20 epochs, respectively. The learning rate was 0.001 for PointNet, PointNet++, and DGCNN and 0.000001 for PointCNN. The batch size of the data was 8 for PointNet, PointCNN, and DGCNN and 32 for PointNet++. All four deep-learning models were trained using a manually labeled dataset of 800 training samples generated from 500 sorghum plants through data augmentation. A test set comprising 48 individual sorghum plants was utilized to evaluate the segmentation results. The training time for the PointNet model was approximately 2 h, with a prediction time of around 25 min for the testing set. Similarly, PointNet++ required around 3 h for training and about 30 min for predicting the testing set. On the other hand, PointCNN took around 3 h and 15 min for training, with a prediction time of approximately 30 min for the testing set. Lastly, DGCNN took training time of around 3 h and 35 min and about 45 min to predict the testing set. PointNet and PointNet++ have relatively fast inference times because these models were designed to process individual point clouds independently. Similarly, PointCNN makes spatially local correlations from point clouds; hence, it has relatively faster inference times than DGCNN. In contrast, DGCNN considers

local neighborhoods of point clouds and builds a graph structure to capture spatial relationships. Therefore, DGCNN involves more complex computations than other models, which take slightly longer inference times. The segmentation results were carried out on a workstation with Intel (R) Xeon (R) Gold 6230 CPU @ 2.10 GHz × 80, 256 GB RAM, and 4 GPUs NVIDIA RTX TITAN 24 GB per GPU.

The segmentation performance evaluation results using all four deep learning models for 48 sorghum testing plants obtained by quantitative indicators are shown in Table II. The PointNet segmentation results of the sorghum plant testing data, the mean recall, precision, F1-score, IoU, and accuracy for stem-leaf-panicle segmentation were 93.7%, 84.0%, 88.3%, 80.2%, and 82.3%, respectively. Likewise, the PointNet++ segmentation results of the test set, the mean recall, precision, F1-score, IoU, and accuracy for stem-leaf-panicle segmentation were 94.9%, 94.2%, 94.8%, 90.7%, and 91.5%, respectively. Similarly, the PointCNN segmentation results of the test set, the mean recall, precision, F1-score, IoU, and accuracy for stem-leaf-panicle segmentation were 94.2%, 91.3%, 92.5%, 86.9%, and 87.9%, respectively. And the DGCNN segmentation results of the test set, the mean recall, precision, F1-score, IoU, and accuracy for stem-leaf-panicle segmentation were 93.3%, 88.4%, 90.7%, 83.6%, and 85.6%, respectively. The segmentation results of a testing plant for all four deep learning models trained with 800 sorghum plants are shown in Fig. 10. Predicted output stem-leaf-panicle segmentation results were correlated with an annotated ground truth testing plant. The precise segmentation results of PointNet++ and PointCNN revealed slight differences, while PointNet and DGCNN showed considerable variations close to the top part of a plant, where leaves grow out from the stem. Fig. 11 visualized the sorghum plant organ (stem-leaf-panicle) segmentation results obtained from deep learning segmentation networks.

Sorghum plant organ (stem-leaf-panicle) segmentation is essential for component plant phenotypic trait extraction from LiDAR 3-D point cloud data. In most existing approaches, the user defines thresholds and customized features, and empirical rules are constructed to segment organs based on these thresholds [22], [94]. The utilized four deep learning models in this paper can directly segment plant organs from LiDAR 3-D point cloud data that contains numbers of sorghum plants of different shapes and sizes. Instead of using user-defined thresholds and empirical rules, these models segment the plant organ by point-based networks. The used models for stem-leaf-panicle segmentation may be preferable to existing methods because they have automatically estimated the acceptable results without requiring time-consuming threshold calibration. An approach to extracting features on multiple scales is essential to account for intra-class size differences, including disparity in stem diameter or panicle length and width, and intra-class geometric discrepancy, including a wide range of curvature on the leaves. The complex plant structure significantly impacts local parts variability, which accompanies different parts close to one another. Therefore, the training dataset must be able to consider various local geometric phenomena, including stems, touching leaves and panicles.

TABLE II
ACCURACY ASSESSMENT OF FOUR DIFFERENT 3D POINT-BASED DEEP LEARNING NETWORKS FOR STEM-LEAF-PANICLE SEGMENTATION OF THE TESTING SET

Segmentation evaluation	PointNet	PointNet++	PointCNN	DGCNN
R_e	Min	92.8	94.4	93.5
	Max	94.6	95.3	94.8
	Mean	93.7	94.9	94.2
P_r	Min	82.1	93.5	90.2
	Max	85.8	94.8	92.4
	Mean	84.0	94.2	91.3
F	Min	87.2	94.3	91.6
	Max	89.4	95.2	93.3
	Mean	88.3	94.8	92.5
IoU	Min	78.8	89.8	86.6
	Max	81.5	91.6	87.3
	Mean	80.2	90.7	86.9
Acc	Min	81.3	90.4	87.4
	Max	83.2	92.5	88.3
	Mean	82.3	91.5	87.9

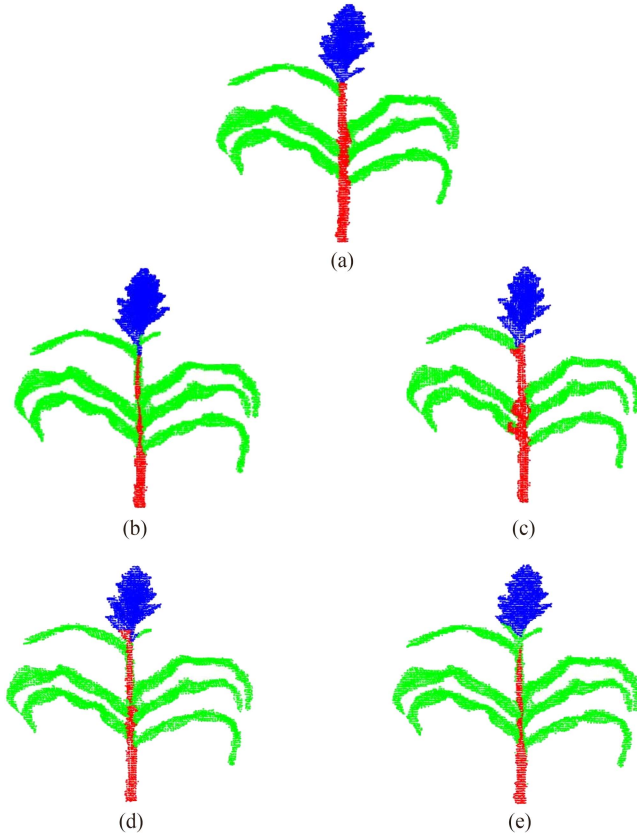


Fig. 10. Sorghum plant segmented using the deep neural networks trained with annotated sorghum plants. (a) Ground truth. (b) PointNet. (c) PointNet++. (d) PointCNN. (e) DGCNN.

The theoretical contributions of all employed four deep learning models for the segmentation of 3-D LiDAR point clouds are as follows.

- 1) PointNet consists of its ability to process unordered point clouds, learn global features independently, utilize shared-weight MLPs, and incorporate a segmentation network.

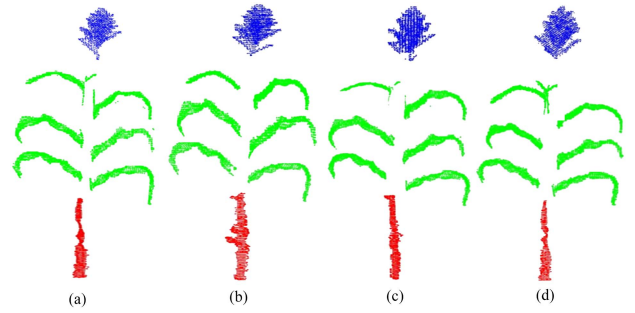


Fig. 11. Visualization of a sorghum plant organ (stem-leaf-panicle) segmentation results obtained using the four deep neural networks: (a) PointNet. (b) PointNet++. (c) PointCNN. (d) DGCNN.

- 2) PointNet++ lies in its hierarchical point cloud processing, the introduction of SA and FP modules for local and global feature learning, and its adaptive feature learning mechanism. These contributions enable PointNet++ to capture complex geometric structures accurately.
- 3) PointCNN comprises its order-independent convolutional operator, adaptive neighborhood learning, feature re-weighting, and point-wise learning and prediction. These contributions enable PointCNN to process unordered point clouds effectively, capture local geometric information, emphasize informative features, and produce accurate segmentation.
- 4) DGCNN incorporates its EdgeConv operations to capture local geometric structures by constructing a local neighborhood dynamic graph and learning pointwise. These theoretical contributions have advanced the field of deep learning-based segmentation and enabled accurate and efficient segmentation of sorghum plants organ from 3D LiDAR point cloud data.

This study performed four notable deep learning models (i.e., PointNet, PointNet++, PointCNN, and DGCNN) for the sorghum plant organ segmentation with different plant heights, leaf numbers, and semi-compact panicles morphology. Out of

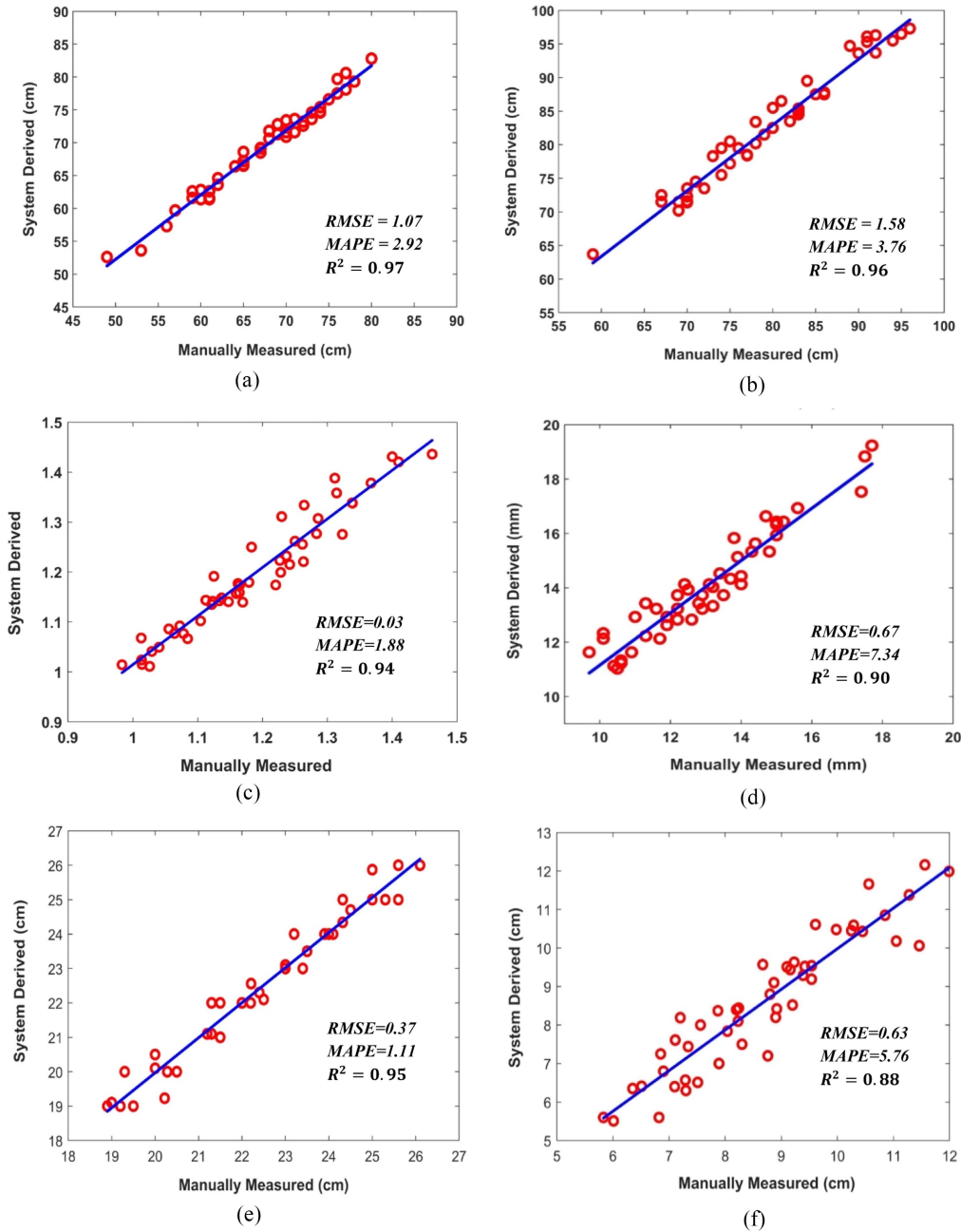


Fig. 12. Comparison of extracted sorghum plant phenotypic traits using PointNet++ deep neural network segmentation model and manually measured values. (a) Plant height, (b) plant crown diameter, (c) plant compactness, (d) stem diameter, (e) panicle length, and (f) panicle width.

these four models, PointNet++ gave the best part segmentation result. However, the PointNet++ segmentation findings have slightly diverged from the ground truth labeled point clouds, generally at the stem-leaf junctions and upper leaf clusters. PointNet model, at the point level, generated 83.2% maximum and 81.3% minimum stem-leaf-panicle segmentation accuracy with a mean accuracy of 82.3%. Similarly, the PointNet++ model estimated 92.5% maximum and 90.4% minimum segmentation accuracy, with a mean accuracy of 91.5%. While the PointCNN model calculated 88.3% maximum and 87.4% minimum segmentation accuracy, with a mean accuracy of 87.9%. Likewise, DGCNN measured 86.7% maximum and 84.5%

minimum segmentation accuracy, with a mean accuracy of 85.6%. The sorghum plant-organ segmentation performance of the three deep learning models (PointNet++, PointCNN, DGCNN) was promising because they have given more than 85% segmentation mean accuracy. In this study PointNet++ model gave more accurate segmentation result as compared to PointCNN and DGCNN; therefore, PointNet++ model's segmentation results were opted for phenotyping traits measurements but may also use the PointCNN and DGCNN models for segmentation and phenotyping traits extraction based on the complexity of point cloud data and the number of training samples. It may require careful hyperparameter tuning to

achieve optimal results. To determine the most appropriate 3D deep learning model for plant-organ segmentation, the specific characteristics of point cloud data, such as point density and objects' complexity, are essential. Overall, plant organ segmentation results propound that the PointNet++ model is robust for various sorghum plants with variable plant heights, growth cycles, leaf counts, and panicles. Although, the PointNet++ segmentation model still has several drawbacks, particularly in segmenting the upper leaf clusters. Because, despite manual observation, determining the topmost point of the sorghum stem is difficult. Thus, a certain amount of model segmentation error of the clusters of the top leaf and estimation of the stem height should be tolerable [68].

B. Phenotypic Trait Extraction

The accuracy evaluation of the extracted phenotypic traits based on the PointNet++ segmentation results was compared to the manually measured trait values. Fig. 12 shows the extracted validation results of six phenotypic traits (i.e., plant height, plant crown diameter, plant compactness, stem diameter, panicle length, and panicle width) for the 48 sorghum testing plant samples. At sorghum plant level, the estimated R^2 of plant height, plant crown diameter, and plant compactness were 0.97, 0.96, and 0.94, respectively. The estimated RMSE of plant height, plant crown diameter, and plant compactness were 1.07, 1.58, and 0.03 cm. The estimated MAPE of plant height, plant crown diameter, and plant compactness were 2.92, 3.76, and 1.88. At sorghum stem level, the estimated R^2 , RMSE and MAPE of stem diameter were 0.90, 0.67 mm, and 7.34, respectively. At sorghum panicle level, the estimated R^2 of panicle length, and panicle width were 0.95 and 0.88, respectively. The estimated RMSE of panicle length, and panicle width were 0.37 and 0.63 cm. And the estimated MAPE of panicle length, and panicle width were 1.11 and 5.76. Extracted phenotypic trait results correlation between the manual measurements for stem diameter, and panicle width were medium, and plant height, plant crown diameter, plant compactness, and panicle length correlations were high.

All the extracted phenotypic traits depend on the point cloud segmentation results at the plant level. Linear regression analysis of the extracted phenotypic traits revealed that the correlation of stem diameter ($R^2 = 0.90$) and panicle width ($R^2 = 0.88$) were slightly lower than the other four parameters. In the case of stem, the obtained slightly lower correlation result may be due to the dissimilarity of the stem diameter size from bottom to top and the segmentation results at the stem-leaf junctions. Similarly in the case of panicle, the attained slightly lower correlation result may be due to the dissimilarity of the panicle width from bottom to top and the semi-compact panicles morphology [95]. The system-derived plant height, plant crown diameter, plant compactness, stem diameter, panicle length and panicle width of sorghum plants were well correlated with the manual measurements because the estimated R^2 were 0.97, 0.96, 0.94, 0.90, 0.95, and 0.88, respectively. The high correlation between system-derived phenotypic traits with manual measurements validates the accuracy and utility of our approach for extracting phenotypic traits.

V. CONCLUSION

This article presents four 3-D point cloud-based deep learning models (i.e., PointNet, PointNet++, PointCNN, and DGCNN) for the segmentation of sorghum plants into their stems, leaves, and panicles. Subsequently, the six-sorghum plant phenotypic traits were extracted using the segmented point clouds. The annotated 3-D point cloud dataset was used for training the deep learning networks. The segmentation results indicate that the performance of the PointNet model was average. With a mean accuracy of 91.5%, the PointNet++ model produced the best segmentation results. This accomplishment of the PointNet++ segmentation model may be because of its simplicity in estimating the hierarchical local region's size needed to feature extraction at multi-scales. The PointCNN and DGCNN models produced good segmentation results. However, defining local regions for extraction of features by K-neighborhood of points is less realistic for modeling the geometry of a plant. Since the ideal K for each scale will rely on the density of the point and the plant part structure's size of the 3-D point cloud. Six phenotypic traits have been measured precisely (i.e., plant height, plant crown diameter, plant compactness, stem diameter, panicle length, and panicle width) using the segmentation results of the PointNet++ model for 48 sorghum plant testing samples. Moreover, the R^2 values for all the phenotypic traits were between 0.88 to 0.97. The sorghum plant phenotypic traits extraction results show that the 3-D point cloud based PointNet++ deep learning segmentation model is well suited for measuring the traits investigated in this study.

ACKNOWLEDGMENT

The data are available in Mendeley Data (an open research data repository) with <https://data.mendeley.com/datasets/pfnfzrmrg7/1>.

REFERENCES

- [1] C. Zhao et al., "Crop phenomics: Current status and perspectives," *Front. Plant Sci.*, vol. 10, Jun. 2019, Art. no. 714, doi: [10.3389/fpls.2019.00714](https://doi.org/10.3389/fpls.2019.00714).
- [2] J. Kumar, A. Pratap, and S. Kumar, *Phenomics in Crop Plants: Trends, Options and Limitations*, vol. 8. Berlin, Germany: Springer-Verlag, 2015.
- [3] D. Houle, D. R. Govindaraju, and S. Omholt, "Phenomics: The next challenge," *Nature Rev. Genet.*, vol. 11, no. 12, pp. 855–866, Dec. 2010, doi: [10.1038/nrg2897](https://doi.org/10.1038/nrg2897).
- [4] M. F. Drecer, G. Molero, C. Rivera-Amado, C. John-Bejai, and Z. Wilson, "Yielding to the image: How phenotyping reproductive growth can assist crop improvement and production," *Plant Sci.*, vol. 282, pp. 73–82, May 2019, doi: [10.1016/j.plantsci.2018.06.008](https://doi.org/10.1016/j.plantsci.2018.06.008).
- [5] D. Reinhardt and C. Kuhlemeier, "Plant architecture," *Eur. Mol. Biol. Org. Rep.*, vol. 3, no. 9, pp. 846–851, Sep. 2002, doi: [10.1093/embo-reports/kvf177](https://doi.org/10.1093/embo-reports/kvf177).
- [6] S. Paulus, "Measuring crops in 3D: Using geometry for plant phenotyping," *Plant Methods*, vol. 15, no. 1, Dec. 2019, Art. no. 103, doi: [10.1186/s13007-019-0490-0](https://doi.org/10.1186/s13007-019-0490-0).
- [7] F. Perez-Sanz, P. J. Navarro, and M. Egea-Cortines, "Plant phenomics: An overview of image acquisition technologies and image data analysis algorithms," *Gigascience*, vol. 6, no. 11, pp. 1–18, Nov. 2017, doi: [10.1093/gigascience/gix092](https://doi.org/10.1093/gigascience/gix092).
- [8] C.-R. Shyu, J. M. Green, D. P. K. Lun, T. Kazic, M. Schaeffer, and E. Coe, "Image analysis for mapping immeasurable phenotypes in maize [life sciences]," *IEEE Signal Process. Mag.*, vol. 24, no. 3, pp. 115–118, May 2007.
- [9] M. Ikeda et al., "Analysis of rice panicle traits and detection of QTLs using an image analyzing method," *Breeding Sci.*, vol. 60, no. 1, pp. 55–64, 2010, doi: [10.1270/jsbbs.60.55](https://doi.org/10.1270/jsbbs.60.55).

- [10] R. T. Clark et al., "Three-dimensional root phenotyping with a novel imaging and software platform," *Plant Physiol.*, vol. 156, no. 2, pp. 455–465, Jun. 2011, doi: [10.1104/pp.110.169102](https://doi.org/10.1104/pp.110.169102).
- [11] V. Hoyos-Villegas, J. H. Houx, S. K. Singh, and F. B. Fritschi, "Ground-based digital imaging as a tool to assess soybean growth and yield," *Crop Sci.*, vol. 54, no. 4, pp. 1756–1768, Jul. 2014, doi: [10.2135/crops.2013.08.0540](https://doi.org/10.2135/crops.2013.08.0540).
- [12] G. Pan, F.-M. Li, and G.-J. Sun, "Digital camera based measurement of crop cover for wheat yield prediction," in *Proc. IEEE Int. Geosci. Remote Sens. Symp.*, 2007, pp. 797–800, doi: [10.1109/IGARSS.2007.4422917](https://doi.org/10.1109/IGARSS.2007.4422917).
- [13] D. Chen et al., "Dissecting the phenotypic components of crop plant growth and drought responses based on high-throughput image analysis," *Plant Cell*, vol. 26, no. 12, pp. 4636–4655, Jan. 2015, doi: [10.1105/tpc.114.129601](https://doi.org/10.1105/tpc.114.129601).
- [14] A.-K. Mahlein, "Plant disease detection by imaging sensors—Parallels and specific demands for precision agriculture and plant phenotyping," *Plant Dis.*, vol. 100, no. 2, pp. 241–251, Feb. 2016, doi: [10.1094/PDIS-03-15-0340-FE](https://doi.org/10.1094/PDIS-03-15-0340-FE).
- [15] L. Li, Q. Zhang, and D. Huang, "A review of imaging techniques for plant phenotyping," *Sensors*, vol. 14, no. 11, pp. 20078–20111, Oct. 2014, doi: [10.3390/s141120078](https://doi.org/10.3390/s141120078).
- [16] R. Qiu et al., "Sensors for measuring plant phenotyping: A review," *Int. J. Agricultural Biol. Eng.*, vol. 11, no. 2, pp. 1–17, 2018, doi: [10.25165/j.ijabe.20181102.2696](https://doi.org/10.25165/j.ijabe.20181102.2696).
- [17] Y. Jiang and C. Li, "Convolutional neural networks for image-based high-throughput plant phenotyping: A review," *Plant Phenomics*, vol. 2020, pp. 1–22, Apr. 2020, doi: [10.34133/2020/4152816](https://doi.org/10.34133/2020/4152816).
- [18] W. Shi, R. van de Zedde, H. Jiang, and G. Kootstra, "Plant-part segmentation using deep learning and multi-view vision," *Biosyst. Eng.*, vol. 187, pp. 81–95, Nov. 2019, doi: [10.1016/j.biosystemseng.2019.08.014](https://doi.org/10.1016/j.biosystemseng.2019.08.014).
- [19] H. Wang, W. Zhang, G. Zhou, G. Yan, and N. Clinton, "Image-based 3D corn reconstruction for retrieval of geometrical structural parameters," *Int. J. Remote Sens.*, vol. 30, no. 20, pp. 5505–5513, Sep. 2009, doi: [10.1080/01431160903130952](https://doi.org/10.1080/01431160903130952).
- [20] W. Yang, L. Duan, G. Chen, L. Xiong, and Q. Liu, "Plant phenomics and high-throughput phenotyping: Accelerating rice functional genomics using multidisciplinary technologies," *Curr. Opin. Plant Biol.*, vol. 16, no. 2, pp. 180–187, May 2013, doi: [10.1016/j.pbi.2013.03.005](https://doi.org/10.1016/j.pbi.2013.03.005).
- [21] Y. Su, Q. Ma, and Q. Guo, "Fine-resolution forest tree height estimation across the Sierra Nevada through the integration of spaceborne LiDAR, airborne LiDAR, and optical imagery," *Int. J. Digit. Earth*, vol. 10, no. 3, pp. 307–323, Mar. 2017, doi: [10.1080/17538947.2016.1227380](https://doi.org/10.1080/17538947.2016.1227380).
- [22] S. Jin et al., "Stem-Leaf segmentation and phenotypic trait extraction of individual maize using terrestrial LiDAR Data," *IEEE Trans. Geosci. Remote Sens.*, vol. 57, no. 3, pp. 1336–1346, Mar. 2019.
- [23] K. Panjwani, A. V. Dinh, and K. A. Wahid, "LiDARPheno—A low-cost LiDAR-based 3D scanning system for leaf morphological trait extraction," *Front. Plant Sci.*, vol. 10, Feb. 2019, Art. no. 147, doi: [10.3389/fpls.2019.00147](https://doi.org/10.3389/fpls.2019.00147).
- [24] L. Lei et al., "Extraction of maize leaf base and inclination angles using terrestrial laser scanning (TLS) data," *IEEE Trans. Geosci. Remote Sens.*, vol. 60, 2022, Art. no. 5701817.
- [25] C. Lin, F. Hu, J. Peng, J. Wang, and R. Zhai, "Segmentation and stratification methods of field maize terrestrial LiDAR point cloud," *Agriculture*, vol. 12, no. 9, Sep. 2022, Art. no. 1450, doi: [10.3390/agriculture12091450](https://doi.org/10.3390/agriculture12091450).
- [26] T. J. Young et al., "Canopy fingerprints" for characterizing three-dimensional point cloud data of soybean canopies," *Front. Plant Sci.*, vol. 14, Mar. 2023, Art. no. 1141153, doi: [10.3389/fpls.2023.1141153](https://doi.org/10.3389/fpls.2023.1141153).
- [27] S. Debnath, M. Paul, and T. Debnath, "Applications of LiDAR in agriculture and future research directions," *J. Imaging*, vol. 9, no. 3, Feb. 2023, Art. no. 57, doi: [10.3390/jimaging9030057](https://doi.org/10.3390/jimaging9030057).
- [28] Q. Guo et al., "Crop 3D—A LiDAR based platform for 3D high-throughput crop phenotyping," *Sci. China Life Sci.*, vol. 61, no. 3, pp. 328–339, Mar. 2018, doi: [10.1007/s11427-017-9056-0](https://doi.org/10.1007/s11427-017-9056-0).
- [29] S. Jin et al., "Deep learning: Individual maize segmentation from terrestrial lidar data using faster R-CNN and regional growth algorithms," *Front. Plant Sci.*, vol. 9, Jun. 2018, Art. no. 866, doi: [10.3389/fpls.2018.00866](https://doi.org/10.3389/fpls.2018.00866).
- [30] S. Sun et al., "In-field high throughput phenotyping and cotton plant growth analysis using LiDAR," *Front. Plant Sci.*, vol. 9, Jan. 2018, Art. no. 16, doi: [10.3389/fpls.2018.00016](https://doi.org/10.3389/fpls.2018.00016).
- [31] L. Xiang, Y. Bao, L. Tang, D. Ortiz, and M. G. Salas-Fernandez, "Automated morphological traits extraction for sorghum plants via 3D point cloud data analysis," *Comput. Electron. Agriculture*, vol. 162, pp. 951–961, Jul. 2019, doi: [10.1016/j.compag.2019.05.043](https://doi.org/10.1016/j.compag.2019.05.043).
- [32] S. Wu et al., "An accurate skeleton extraction approach from 3D point clouds of maize plants," *Front. Plant Sci.*, vol. 10, Mar. 2019, Art. no. 248, doi: [10.3389/fpls.2019.00248](https://doi.org/10.3389/fpls.2019.00248).
- [33] F. Liu et al., "Canopy occupation volume as an indicator of canopy photosynthetic capacity," *New Phytologist*, vol. 232, no. 2, pp. 941–956, Oct. 2021, doi: [10.1111/nph.17611](https://doi.org/10.1111/nph.17611).
- [34] T. Miao et al., "Automatic stem-leaf segmentation of maize shoots using three-dimensional point cloud," *Comput. Electron. Agriculture*, vol. 187, Aug. 2021, Art. no. 106310, doi: [10.1016/j.compag.2021.106310](https://doi.org/10.1016/j.compag.2021.106310).
- [35] D. Wang et al., "DFSP: A fast and automatic distance field-based stem-leaf segmentation pipeline for point cloud of maize shoot," *Front. Plant Sci.*, vol. 14, Jan. 2023, Art. no. 1109314, doi: [10.3389/fpls.2023.1109314](https://doi.org/10.3389/fpls.2023.1109314).
- [36] S. Jin et al., "Lidar sheds new light on plant phenomics for plant breeding and management: Recent advances and future prospects," *Int. Soc. Photogrammetry Remote Sens. J. Photogrammetry Remote Sens.*, vol. 171, pp. 202–223, Jan. 2021, doi: [10.1016/j.isprsjprs.2020.11.006](https://doi.org/10.1016/j.isprsjprs.2020.11.006).
- [37] G. Rivera, R. Porras, R. Florencia, and J. P. Sánchez-Solís, "LiDAR applications in precision agriculture for cultivating crops: A review of recent advances," *Comput. Electron. Agriculture*, vol. 207, Apr. 2023, Art. no. 107737, doi: [10.1016/j.compag.2023.107737](https://doi.org/10.1016/j.compag.2023.107737).
- [38] J. Barker et al., "Development of a field-based high-throughput mobile phenotyping platform," *Comput. Electron. Agriculture*, vol. 122, pp. 74–85, Mar. 2016, doi: [10.1016/j.compag.2016.01.017](https://doi.org/10.1016/j.compag.2016.01.017).
- [39] A. Chaudhury et al., "Machine vision system for 3D plant phenotyping," *IEEE/Assoc. Comput. Machinery Trans. Comput. Biol. Bioinf.*, vol. 16, no. 6, pp. 2009–2022, Nov./Dec. 2019.
- [40] J. Zhou, X. Fu, S. Zhou, J. Zhou, H. Ye, and H. T. Nguyen, "Automated segmentation of soybean plants from 3D point cloud using machine learning," *Comput. Electron. Agriculture*, vol. 162, pp. 143–153, Jul. 2019, doi: [10.1016/j.compag.2019.04.014](https://doi.org/10.1016/j.compag.2019.04.014).
- [41] S. Zhou, X. Chai, Z. Yang, H. Wang, C. Yang, and T. Sun, "Maize-IAS: A maize image analysis software using deep learning for high-throughput plant phenotyping," *Plant Methods*, vol. 17, no. 1, Dec. 2021, Art. no. 48, doi: [10.1186/s13007-021-00747-0](https://doi.org/10.1186/s13007-021-00747-0).
- [42] S. Arya, K. S. Sandhu, J. Singh, and S. Kumar, "Deep learning: As the new frontier in high-throughput plant phenotyping," *Euphytica*, vol. 218, no. 4, Apr. 2022, Art. no. 47, doi: [10.1007/s10681-022-02992-3](https://doi.org/10.1007/s10681-022-02992-3).
- [43] A. Cardellicchio et al., "Detection of tomato plant phenotyping traits using YOLOv5-based single stage detectors," *Comput. Electron. Agriculture*, vol. 207, Apr. 2023, Art. no. 107757, doi: [10.1016/j.compag.2023.107757](https://doi.org/10.1016/j.compag.2023.107757).
- [44] V. N. Balasubramanian, W. Guo, A. L. Chandra, and S. V. Desai, "Computer vision with deep learning for plant phenotyping in agriculture: A survey," *Adv. Comput. Commun.*, vol. 4, no. 2, Jun. 2020, doi: [10.34048/ACC.2020.1.F1](https://doi.org/10.34048/ACC.2020.1.F1).
- [45] S. Kolhar and J. Jagtap, "Plant trait estimation and classification studies in plant phenotyping using machine vision—A review," *Inf. Process. Agriculture*, vol. 10, no. 1, pp. 114–135, Mar. 2023, doi: [10.1016/j.inpa.2021.02.006](https://doi.org/10.1016/j.inpa.2021.02.006).
- [46] L. Xiang and D. Wang, "A review of three-dimensional vision techniques in food and agriculture applications," *Smart Agricultural Technol.*, vol. 5, Oct. 2023, Art. no. 100259, doi: [10.1016/j.atech.2023.100259](https://doi.org/10.1016/j.atech.2023.100259).
- [47] Z. Li, R. Guo, M. Li, Y. Chen, and G. Li, "A review of computer vision technologies for plant phenotyping," *Comput. Electron. Agriculture*, vol. 176, Sep. 2020, Art. no. 105672, doi: [10.1016/j.compag.2020.105672](https://doi.org/10.1016/j.compag.2020.105672).
- [48] M. E. Ghanem, H. Marrou, and T. R. Sinclair, "Physiological phenotyping of plants for crop improvement," *Trends Plant Sci.*, vol. 20, no. 3, pp. 139–144, Mar. 2015, doi: [10.1016/j.tplants.2014.11.006](https://doi.org/10.1016/j.tplants.2014.11.006).
- [49] Y. Lin, "LiDAR: An important tool for next-generation phenotyping technology of high potential for plant phenomics?," *Comput. Electron. Agriculture*, vol. 119, pp. 61–73, Nov. 2015, doi: [10.1016/j.compag.2015.10.011](https://doi.org/10.1016/j.compag.2015.10.011).
- [50] J. Li and L. Tang, "Developing a low-cost 3D plant morphological traits characterization system," *Comput. Electron. Agriculture*, vol. 143, pp. 1–13, Dec. 2017, doi: [10.1016/j.compag.2017.09.025](https://doi.org/10.1016/j.compag.2017.09.025).
- [51] C. Hu, P. Li, and Z. Pan, "Phenotyping of poplar seedling leaves based on a 3D visualization method," *Int. J. Agricultural Biol. Eng.*, vol. 11, no. 6, pp. 145–151, 2018, doi: [10.25165/j.ijabe.20181106.4110](https://doi.org/10.25165/j.ijabe.20181106.4110).
- [52] S. Wu et al., "MVS-Pheno: A portable and low-cost phenotyping platform for maize shoots using multiview stereo 3D reconstruction," *Plant Phenomics*, vol. 2020, pp. 1–17, Mar. 2020, doi: [10.34133/2020/1848437](https://doi.org/10.34133/2020/1848437).
- [53] Y. Wang et al., "Maize plant phenotyping: Comparing 3D laser scanning, multi-view stereo reconstruction, and 3D digitizing estimates," *Remote Sens. (Basel)*, vol. 11, no. 1, Dec. 2018, Art. no. 63, doi: [10.3390/rs11010063](https://doi.org/10.3390/rs11010063).

- [54] Q. Qiu et al., "Field-based high-throughput phenotyping for maize plant using 3D LiDAR point cloud generated with a 'phenomobile,'" *Front. Plant Sci.*, vol. 10, May 2019, Art. no. 554, doi: [10.3389/fpls.2019.00554](https://doi.org/10.3389/fpls.2019.00554).
- [55] S. Madec et al., "High-throughput phenotyping of plant height: Comparing unmanned aerial vehicles and ground LiDAR estimates," *Front. Plant Sci.*, vol. 8, Nov. 2017, Art. no. 2002, doi: [10.3389/fpls.2017.02002](https://doi.org/10.3389/fpls.2017.02002).
- [56] S. Paulus, J. Dupuis, S. Riedel, and H. Kuhlmann, "Automated analysis of barley organs using 3D laser scanning: An approach for high throughput phenotyping," *Sensors*, vol. 14, no. 7, pp. 12670–12686, Jul. 2014, doi: [10.3390/s140712670](https://doi.org/10.3390/s140712670).
- [57] S. Paulus, J. Dupuis, A.-K. Mahlein, and H. Kuhlmann, "Surface feature based classification of plant organs from 3D laserscanned point clouds for plant phenotyping," *BioMed Central Bioinform.*, vol. 14, no. 1, Dec. 2013, Art. no. 238, doi: [10.1186/1471-2105-14-238](https://doi.org/10.1186/1471-2105-14-238).
- [58] S. D. Choudhury, S. Maturu, A. Samal, V. Stoerger, and T. Awada, "Leveraging image analysis to compute 3D plant phenotypes based on voxel-grid plant reconstruction," *Front. Plant Sci.*, vol. 11, Dec. 2020, Art. no. 521431, doi: [10.3389/fpls.2020.521431](https://doi.org/10.3389/fpls.2020.521431).
- [59] J. D. C. Walter, J. Edwards, G. McDonald, and H. Kuchel, "Estimating biomass and canopy height with LiDAR for field crop breeding," *Front. Plant Sci.*, vol. 10, Sep. 2019, Art. no. 1145, doi: [10.3389/fpls.2019.01145](https://doi.org/10.3389/fpls.2019.01145).
- [60] X. Yang et al., "Three-dimensional forest reconstruction and structural parameter retrievals using a terrestrial full-waveform lidar instrument (Echidna)," *Remote Sens. Environ.*, vol. 135, pp. 36–51, Aug. 2013, doi: [10.1016/j.rse.2013.03.020](https://doi.org/10.1016/j.rse.2013.03.020).
- [61] J. Wu, K. Cawse-Nicholson, and J. van Aardt, "3D tree reconstruction from simulated small footprint waveform LiDAR," *Photogrammetric Eng. Remote Sens.*, vol. 79, no. 12, pp. 1147–1157, Dec. 2013, doi: [10.14358/PERS.79.12.1147](https://doi.org/10.14358/PERS.79.12.1147).
- [62] I. Ziamtsov and S. Navlakha, "Plant 3D (P3D): A plant phenotyping toolkit for 3D point clouds," *Bioinformatics*, vol. 36, no. 12, pp. 3949–3950, Jun. 2020, doi: [10.1093/bioinformatics/btaa220](https://doi.org/10.1093/bioinformatics/btaa220).
- [63] A. Singh, B. Ganapathysubramanian, A. K. Singh, and S. Sarkar, "Machine learning for high-throughput stress phenotyping in plants," *Trends Plant Sci.*, vol. 21, no. 2, pp. 110–124, Feb. 2016, doi: [10.1016/j.tplants.2015.10.015](https://doi.org/10.1016/j.tplants.2015.10.015).
- [64] I. Ziamtsov and S. Navlakha, "Machine learning approaches to improve three basic plant phenotyping tasks using three-dimensional point clouds," *Plant Physiol.*, vol. 181, no. 4, pp. 1425–1440, Dec. 2019, doi: [10.1104/pp.19.00524](https://doi.org/10.1104/pp.19.00524).
- [65] K. Mochida et al., "Computer vision-based phenotyping for improvement of plant productivity: A machine learning perspective," *GigaScience*, vol. 8, no. 1, Jan. 2019, Art. no. giy153, doi: [10.1093/gigascience/giy153](https://doi.org/10.1093/gigascience/giy153).
- [66] J. R. Ubbens and I. Stavness, "Corrigendum: Deep plant phenomics: A deep learning platform for complex plant phenotyping tasks," *Front. Plant Sci.*, vol. 8, Jan. 2018, Art. no. 1190, doi: [10.3389/fpls.2017.02245](https://doi.org/10.3389/fpls.2017.02245).
- [67] Z. Ao et al., "Automatic segmentation of stem and leaf components and individual maize plants in field terrestrial LiDAR data using convolutional neural networks," *Crop J.*, vol. 10, no. 5, pp. 1239–1250, Dec. 2021, doi: [10.1016/j.cj.2021.10.010](https://doi.org/10.1016/j.cj.2021.10.010).
- [68] Y. Li et al., "Automatic organ-level point cloud segmentation of maize shoots by integrating high-throughput data acquisition and deep learning," *Comput. Electron. Agriculture*, vol. 193, Feb. 2022, Art. no. 106702, doi: [10.1016/j.compag.2022.106702](https://doi.org/10.1016/j.compag.2022.106702).
- [69] F. P. Boogaard, E. J. van Henten, and G. Kootstra, "Improved point-cloud segmentation for plant phenotyping through class-dependent sampling of training data to battle class imbalance," *Front. Plant Sci.*, vol. 13, Mar. 2022, Art. no. 838190, doi: [10.3389/fpls.2022.838190](https://doi.org/10.3389/fpls.2022.838190).
- [70] F. P. Boogaard, E. J. van Henten, and G. Kootstra, "Boosting plant-part segmentation of cucumber plants by enriching incomplete 3D point clouds with spectral data," *Biosyst. Eng.*, vol. 211, pp. 167–182, Nov. 2021, doi: [10.1016/j.biosystemseng.2021.09.004](https://doi.org/10.1016/j.biosystemseng.2021.09.004).
- [71] S. Jin et al., "Separating the structural components of maize for field phenotyping using terrestrial LiDAR data and deep convolutional neural networks," *IEEE Trans. Geosci. Remote Sens.*, vol. 58, no. 4, pp. 2644–2658, Apr. 2020.
- [72] W. Liu, J. Sun, W. Li, T. Hu, and P. Wang, "Deep learning on point clouds and its application: A survey," *Sensors*, vol. 19, no. 19, Sep. 2019, Art. no. 4188, doi: [10.3390/s19194188](https://doi.org/10.3390/s19194188).
- [73] G. Bernotas et al., "A photometric stereo-based 3D imaging system using computer vision and deep learning for tracking plant growth," *GigaScience*, vol. 8, no. 5, May 2019, Art. no. giz056, doi: [10.1093/gigascience/giz056](https://doi.org/10.1093/gigascience/giz056).
- [74] K. Turgut, H. Dutagaci, G. Galopin, and D. Rousseau, "Segmentation of structural parts of rosebush plants with 3D point-based deep learning methods," *Plant Methods*, vol. 18, no. 1, Dec. 2022, Art. no. 20, doi: [10.1186/s13007-022-00857-3](https://doi.org/10.1186/s13007-022-00857-3).
- [75] D. Li, J. Li, S. Xiang, and A. Pan, "PSegNet: Simultaneous semantic and instance segmentation for point clouds of plants," *Plant Phenomics*, vol. 2022, pp. 1–20, May 2022, doi: [10.34133/2022/9787643](https://doi.org/10.34133/2022/9787643).
- [76] D. Li et al., "PlantNet: A dual-function point cloud segmentation network for multiple plant species," *Int. Soc. Photogrammetry Remote Sens. J. Photogrammetry Remote Sens.*, vol. 184, pp. 243–263, Feb. 2022, doi: [10.1016/j.isprsjprs.2022.01.007](https://doi.org/10.1016/j.isprsjprs.2022.01.007).
- [77] S. Li, L. Dai, H. Wang, Y. Wang, Z. He, and S. Lin, "Estimating leaf area density of individual trees using the point cloud segmentation of terrestrial LiDAR data and a voxel-based model," *Remote Sens. (Basel)*, vol. 9, no. 11, Nov. 2017, Art. no. 1202, doi: [10.3390/rs911202](https://doi.org/10.3390/rs911202).
- [78] T. Duan, S. C. Chapman, E. Holland, G. J. Rebetzke, Y. Guo, and B. Zheng, "Dynamic quantification of canopy structure to characterize early plant vigour in wheat genotypes," *J. Exp. Botany*, vol. 67, no. 15, pp. 4523–4534, Aug. 2016, doi: [10.1093/jxb/erw227](https://doi.org/10.1093/jxb/erw227).
- [79] R. Du, Z. Ma, P. Xie, Y. He, and H. Cen, "PST: Plant segmentation transformer for 3D point clouds of rapeseed plants at the podding stage," *Int. Soc. Photogrammetry Remote Sens. J. Photogrammetry Remote Sens.*, vol. 195, pp. 380–392, Jan. 2023, doi: [10.1016/j.isprsjprs.2022.11.022](https://doi.org/10.1016/j.isprsjprs.2022.11.022).
- [80] Q. Guo et al., "Application of deep learning in ecological resource research: Theories, methods, and challenges," *Sci. China Life Sci.*, vol. 63, no. 10, pp. 1457–1474, Oct. 2020, doi: [10.1007/s11430-019-9584-9](https://doi.org/10.1007/s11430-019-9584-9).
- [81] D. Griffiths and J. Boehm, "A review on deep learning techniques for 3D sensed data classification," *Remote Sens. (Basel)*, vol. 11, no. 12, Jun. 2019, Art. no. 1499, doi: [10.3390/rs11121499](https://doi.org/10.3390/rs11121499).
- [82] B. Li and C. Guo, "MASPC Transform: A plant point cloud segmentation network based on multi-head attention separation and position code," *Sensors*, vol. 22, no. 23, Nov. 2022, Art. no. 9225, doi: [10.3390/s22239225](https://doi.org/10.3390/s22239225).
- [83] K. Turgut, H. Dutagaci, and D. Rousseau, "RoseSegNet: An attention-based deep learning architecture for organ segmentation of plants," *Biosyst. Eng.*, vol. 221, pp. 138–153, Sep. 2022, doi: [10.1016/j.biosystemseng.2022.06.016](https://doi.org/10.1016/j.biosystemseng.2022.06.016).
- [84] E. Marks et al., "High precision leaf instance segmentation for phenotyping in point clouds obtained under real field conditions," *IEEE Robot. Automat. Lett.*, vol. 8, no. 8, pp. 4791–4798, Aug. 2023.
- [85] S. Zheng, J. Pan, C. Lu, and G. Gupta, "PointNorm: Dual normalization is all you need for point cloud analysis," 2022, *arXiv:2207.06324*.
- [86] CloudCompare, "Cloud Compare (version 2.10.2) (2.10.2)," 2019. [Online]. Available: <http://www.cloudcompare.org/>
- [87] R. Q. Charles, H. Su, M. Kaichun, and L. J. Guibas, "PointNet: Deep learning on point sets for 3D classification and segmentation," in *Proc. IEEE Conf. Comput. Vis. Pattern Recognit.*, 2017, pp. 652–660, doi: [10.1109/CVPR.2017.16](https://doi.org/10.1109/CVPR.2017.16).
- [88] C. R. Qi, L. Yi, H. Su, and L. J. Guibas, "PointNet++: Deep hierarchical feature learning on point sets in a metric space," *Adv. Neural Inf. Process. Syst.*, vol. 30, pp. 5099–5108, Jun. 2017.
- [89] Y. Li, R. Bu, M. Sun, W. Wu, X. Di, and B. Chen, "PointCNN: Convolution on X-transformed points," in *Proc. Int. Conf. Neural Inf. Process. Syst.*, vol. 31, Jan. 2018, pp. 828–838.
- [90] Y. Wang, Y. Sun, Z. Liu, S. E. Sarma, M. M. Bronstein, and J. M. Solomon, "Dynamic graph CNN for learning on point clouds," *Assoc. Comput. Machinery Trans. Graph.*, vol. 38, no. 5, pp. 1–12, Nov. 2019, doi: [10.1145/3326362](https://doi.org/10.1145/3326362).
- [91] C. Goutte and E. Gaussier, "A probabilistic interpretation of precision, recall and f-score, with implication for evaluation," *Adv. Inf. Retrieval*, vol. 3408, pp. 345–359, 2005.
- [92] G. Bradski and A. Kaehler, *Learning OpenCV: Computer Vision With the OpenCV Library*. Sebastopol, CA, USA: O'Reilly Media, Inc, 2008.
- [93] A. Fitzgibbon, M. Pilu, and R. B. Fisher, "Direct least square fitting of ellipses," *IEEE Trans. Pattern Anal. Mach. Intell.*, vol. 21, no. 5, pp. 476–480, May 1999.
- [94] S. Thapa, F. Zhu, H. Walia, H. Yu, and Y. Ge, "A novel LiDAR-based instrument for high-throughput, 3D measurement of morphological traits in maize and sorghum," *Sensors*, vol. 18, no. 4, Apr. 2018, Art. no. 1187, doi: [10.3390/s18041187](https://doi.org/10.3390/s18041187).
- [95] L. Wang et al., "Genome-wide association mapping identifies novel panicle morphology loci and candidate genes in sorghum," *Front. Plant Sci.*, vol. 12, Oct. 2021, Art. no. 743838, doi: [10.3389/fpls.2021.743838](https://doi.org/10.3389/fpls.2021.743838).

Ajay Kumar Patel (Student Member, IEEE) received the B.S. degree in electronics and communications engineering from Rajiv Gandhi Technical University, Bhopal, India, in 2009, the M.S. degree in geoinformatics and natural resources engineering from the Indian Institute of Technology, Bombay, India, in 2013, and the Ph.D. degree in geomatics engineering from the Indian Institute of Technology Roorkee, Roorkee, India, in 2021.

He joined the Department of Smart Agricultural Systems, Chungnam National University Daejeon, South Korea, in 2022 as a Postdoctoral Researcher. His research interests include processing of remote sensing imageries (satellite/airborne/UAV), RGB/multispectral/hyperspectral/LiDAR remote sensing, and plant phenotyping from 3-D LiDAR point cloud datasets using deep learning techniques.

Eun-Sung Park received the B.S. degree in agriculture from the School of Applied Bioscience, Kyungpook National University, Daegu, South Korea, in 2019, and the M.S. degree in engineering from the Department of Smart Agriculture Systems, Chungnam National University, Daejeon, in 2022.

His research interests include plant phenotyping from 3-D LiDAR point cloud datasets and image processing.

Hongseok Lee received the B.S., M.S., and Ph.D. degrees in biosystems machinery engineering from Chungnam National University, Daejeon, South Korea, in 2013, 2015, and 2022, respectively.

He is working with Korea-NICS(National Institute of Crop Science and Technology), Miryang, South Korea, as a Scientist since July 2020. His research interests include development of field crop Big Data analysis algorithm.

G. G. Lakshmi Priya received the B.S. degree in computer science from Periyar University, Salem, India, in 2001, the M.C.A. and M.Phil. degrees in computer science from Bharathiar University, Coimbatore, India, in 2004 and 2009, respectively, and the Ph.D. degree in computer applications from the Department of Computer Applications, National Institute of Technology, Tiruchirappalli, India, in 2014.

She joined the School of Information Technology and Engineering, Vellore Institute of Technology, Vellore, India, in 2014. Since 2018, she has been an Associate Professor and Head of the Department of Multimedia, Vellore Institute of Technology. Her research interests include computing, machine learning, programming, image processing, and business intelligence.

Hangi Kim received the B.S. degree in biosystems machinery engineering and computer convergence and the M.S. degree in biosystems machinery engineering from Chungnam National University, Daejeon, South Korea, in 2020 and 2022, respectively.

His research interests include employing deep learning techniques for plant phenomics, focusing on hyperspectral and multispectral imaging.

Rahul Joshi received the B.S. degree in chemistry, physics, and mathematics from Kumaun University, Nainital, India, in 2013, and the M.S. degree in biosystems machinery engineering from Chungnam National University, Daejeon, South Korea, in 2018.

His research interests include quality measurement of agricultural products based on nondestructive spectral analysis.

Muhammad Akbar Andi Arief received the B.S. degree in agricultural and machinery engineering from the Faculty of Agricultural Technology, Universitas Gadjah Mada, Yogyakarta, Indonesia, in 2020, and the M.S. degree in smart agriculture systems from Chungnam National University, Daejeon, South Korea, in 2023.

He worked as a Field Assistant in an irrigation modernization project and as a Research Assistant in the Smart Agriculture Research Group, Universitas Gadjah Mada. His research interests include non-destructive measurement, plant phenotyping and image processing.

Moon S. Kim received the B.S. degree in mathematics/physics, M.S. degree in geography/remote sensing, and Ph.D. degree in natural resource sciences from the University of Maryland, College Park, MD, USA, in 1988, 1994, and 1999, respectively.

He joined ARS, USDA in 1999 as a research Physicist working on development of optical sensing technologies for food safety research projects. Prior to joining ARS-USDA, he held professional positions at NASA/GSFC, Greenbelt, MD for over 10 years. He leads a multidisciplinary team of researchers to develop innovative sensing methodologies and technologies to address food safety concerns for food production and to aid in reducing food safety risks in food processing.

Insuck Baek received the B.S. and M.S. degrees in biosystems machinery engineering from Chungnam National University, Daejeon, South Korea, in 2010 and 2012, respectively, and the Ph.D. degree from the University of Maryland, Baltimore, MD, USA, in 2019.

He has been working with USDA-ARS, Beltsville, MD, USA, as a Scientist since February 2023. His research interests include machine vision and hyperspectral imaging for quality and safety evaluation of agricultural and food materials.

Byoung-Kwan Cho received the B.S. and M.S. degrees in agricultural machinery engineering from the Department of Agricultural Engineering, Seoul National University, Seoul, South Korea, in 1993 and 1998, respectively, and the Ph.D. degree in agricultural and biological engineering from the Department of Agricultural and Biological Engineering, the Pennsylvania State University, University Park, PA, USA, in 2003.

He joined the Department of Agricultural and Biological Engineering, Purdue University, West Lafayette, IN, USA, in 2003, and ARS, USDA, Beltsville, MD, USA, in 2005, as a Postdoctoral Researcher. Since 2006 he has been a Professor with the Department of Biosystems Machinery Engineering, Chungnam National University, Daejeon, South Korea. His research interests include nondestructive biosensing for quality and safety evaluation of agricultural and food materials.